Confocal microscopy and passive staining with the styryl dye FM1-43: a convenient method to evaluate morphometric changes in nodes of Ranvier of single living myelinated axons

E. Benoit*[,1,2], C. Mattei[3], S. C. Brown[4] and **J. Molgò[1,2]**

[1] Institut des Neurosciences Paris-Saclay, UMR CNRS/Université Paris-Sud 9197, CNRS, 91198 Gif-sur-Yvette, France
[2] Service d'Ingénierie Moléculaire des Protéines (DRF/iBiTec-S/SIMOPRO), CEA of Saclay, 91191 Gif-sur-Yvette, France
[3] Laboratoire Mitovasc, UMR CNRS 6214 INSERM 1083, Université d'Angers, 49045 Angers, France
[4] Institut des Sciences du Végétal, UPR CNRS 2355, CNRS, 91198 Gif-sur-Yvette, France

Confocal laser scanning microscopy was used to image at high resolution single living myelinated axons isolated from the frog sciatic nerve. Before imaging, the nerve fibres were exposed to the fluorescent styryl dye FM1-43 and thereafter rinsed with dye-free solution. This procedure, which consistently stained nerve membranes for several hours, was particularly useful and especially adapted for delineating the contours of the node of Ranvier and revealing the myelin sheath layers surrounding the axon. Images of three-dimensional digital reconstructions of the structure of a single myelinated axon were obtained by "look-through" projections from series of optical sections through the axon, collected before and during various treatments. Results were quantified, on the same myelinated axon, by measuring the internodal diameter, the nodal length (L) and the nodal diameter (D) and then by calculating the nodal volume (V) as: $V = \pi L (D/2)^2$, assuming the simplest geometry in which a node of Ranvier approaches a cylinder. This method is of particular interest since it provides the possibility to detect and quantify changes in nodal volume of a given living myelinated axon under various experimental conditions. Results previously obtained with this method are shown.

Keywords: neuromorphology; cell volume; nodes of Ranvier of myelinated nerve fibres; FM1-43; confocal laser scanning microscopy

1. Type of research

This type of research aims detecting alterations of nerve cell morphology under physiological or pathological conditions. It consists in visualising living nerve membranes by means of fluorescence and quantifying time-dependent changes of nerve cell volume on the same single preparation during various experimental treatments. Frog myelinated axons are exemplified as nerve cells in this chapter knowing that this method can be applied to any nerve cell.

2. Time required

In general, 4-6 teased apart myelinated axons can be simultaneously studied in a single experiment. The time required to run the whole protocol on these nerve fibres is between 4 and 7 hours. This time is subdivided into the four following phases.

-Forty minutes for myelinated axon dissection, including sacrifice of the frog and sciatic nerve isolation.

-Twenty minutes to stain nerve fibres with FM1-43.

-Three to five minutes to conduct confocal laser scanning microscopy, including collecting a series of optical sections of a myelinated axon and obtaining the three-dimensional reconstruction of its structure by a "look-through" projection. The time is typically between 1 and 3 hours to monitor a whole experiment of changes in nodal volume produced by the different experimental conditions.

-The time required for data analysis of an experiment depends on the number of data sets (*i.e.* the number of image stacks) recorded for a given myelinated axon, as well as on the number of myelinated axons simultaneously studied. In general, 2 hours are required to calculate the changes in nodal volume of 4-6 different axons.

3. Materials

Adult double pithed male frogs (*Rana temporaria*) weighing 20-30 g were used for the experiments. The standard physiological solution had the following composition (in mM): NaCI, 111.5; KCI, 2.5; $CaCI_2$, 1.8; N-2-hydroxyethylpiperazine-N'-2-ethane-sulphonic acid (HEPES), 10 (buffered at pH 7.4 with NaOH). All chemicals were purchased from Sigma-Aldrich Chimie (St. Quentin Fallavier, France).

To achieve the dissection procedure of myelinated nerve fibres, the following materials are needed: (1) A dissection glass plate (l x w: about 5 x 7 cm), (2) a microscope (Carl Zeiss, Jena, Germany) equipped with x10 objective lens, (3) knee-bent scissors (F. Tuscher, Bern, Switzerland), (4) tweezers (style #5, 110 mm; Sigma-Aldrich Chimie, St. Quentin

Fallavier, France), (5) a Rhodorsil®-lined (Silicone, about 2 mm thick) Plexiglas chamber (l x w x h: about 30 x 40 x 5 mm), and (6) Fine entomological pins " minutiae " (diameter: 0.15 mm; Boubé, Paris, France).

Image acquisition and analysis of myelinated nerve fibres are performed using a fluorescent dye, a confocal laser scanning system and a workstation. The fluorescent styryl dye, *N*-(3-triethylammoniumpropyl)-4-(*p*-dibutylaminostyryl) pyridinium dibromide (FM1-43, molecular weight of 611.6), was stored at -20°C as 10 µL aliquots of a 1 mM solution in distilled water and used at 2 µM in the standard physiological solution (Molecular Probes Europe BV, Leiden, The Netherlands). Aliquots may be kept at 4°C during experiments and are unstable at room temperature.

A Sarastro-2000 confocal laser scanning system (Molecular Dynamics, Sunnyvale, CA, USA), using an Argon laser and an upright Nikon Optiphot-2 microscope equipped with a x40, 0.75 NA water-immersion no-coverslip objective (Zeiss; 2 mm working-distance), was employed. A SiliconGraphics Personal Iris 4D/35 workstation (Mountain View, CA, USA), using a UNIX operating system and the software ImageSpace (version 3.2, Molecular Dynamics, Sunnyvale, CA, USA), integrated into the Sarastro system, allowed controlling the scanner module and image analysis.

More specific to the results exemplified in this report, Pacific ciguatoxin (P-CTX-1B), D-mannitol and tetrodotoxin (TTX) were used. P-CTX-1B (molecular weight 1111 Da) was extracted from poisonous moray eels (*Gymnothorax javanicus*) and purified to homogeneity (kindly provided by Dr. A.M. Legrand, Unité d'Océanographie Médicale, Institut Territorial de Recherches Louis Malardé, Papeete, Tahiti, Polynésie Française). The dry toxic extracts were dissolved in ethanol. The solution thus obtained was aliquoted and the ethanol was evaporated under nitrogen flux to dryness. Dried samples were kept at -20°C and dissolved immediately before experiments in the standard physiological solution to give a final toxin concentration of 10 nM. D-mannitol (Sigma-Aldrich Chimie, St. Quentin Fallavier, France) was used at 100 mM concentration to increase the osmolality of the external solution by 48 %. The osmolality of solutions was determined by using a freezing point osmometer (Knauer, Berlin, Germany). TTX (Sigma-Aldrich Chimie, St. Quentin Fallavier, France) was used at 1 µM concentration to block voltage-dependent sodium channels, and dissolved in the standard physiological solution.

4. Detailed procedure

4.1 Dissection procedure of myelinated nerve fibres

All efforts were made to minimise animal suffering. The frog was first decapitated and demedullated. Then the two posterior legs were cut. After removing the skin, one leg was placed in a glass dish filled with the standard physiological solution and kept in a refrigerator for further experiments, while the second one was immediately used for the dissection of myelinated nerve fibres. For this purpose, both a piece of the sciatic nerve of about 3 cm length and the *gastrocnemius* muscle were rapidly removed from the leg and mounted on the dissection glass plate placed under the Zeiss microscope. The nerve trunk was continuously covered by the standard physiological solution throughout the whole dissection procedure performed at room temperature (22-24°C).

The sciatic nerve innervating the *gastrocnemius* muscle comprises two main nerves, the peroneal nerve and the tibial nerve ending with several small branches, one of them being the motor branch reaching the top of the muscle (Fig. 1A). The nerve fibre fascicles are surrounded like a sleeve by a sheath of lamellar connective tissue in the epineurium and perineurium, consisting partly of continuous sheets of cellular processes closely linked by tight junctions. The next step of the dissection procedure was to remove this sheath which covers the entire course of the sciatic nerve, branching as the nerve branches even to single fibres and ending only just at the nerve fibre terminal. For this, branching nerve trunks are preferable to open the sheath (epineurium and perineurium) since it is much easier when started from a cut branch of a nerve trunk. Hence, the sheath was opened with knee-bent scissors along the peroneal and tibial nerves starting from an incision at the separation level of these two nerves (Fig. 1B), moved to one side and cut (Fig. 1C). Then, using tweezers, the peroneal nerve was carefully pulled away while simultaneously the tibial nerve was pulled in the opposite direction, to avoid stretching the fibres (Fig. 1D). For the following steps, a de-sheathed piece of either the peroneal or the tibial nerve may be used.

With fine entomological pins and tweezers, the de-sheathed piece of nerve was pinned to the bottom of the Plexiglas chamber, filled with the standard physiological solution, and myelinated nerve fibres were gently teased apart to form a fan (Fig. 1E).

4.2 Staining procedure of myelinated nerve fibres

Before imaging, the plasma membrane of myelinated axons was stained with the fluorescent styryl dye FM1-43. For this purpose, preparations were exposed, without light and for 15 min, to FM1-43 (2 µM final concentration) dissolved in 2 mL standard physiological solution, and thereafter rinsed thoroughly several times with a dye-free solution.

4.3 Acquisition procedure for images of myelinated nerve fibres

The chamber, filled with 1.5 mL standard physiological solution, was set on a microscope slide (l x w x h: 25 x 75 x 1 mm) as a support under the upright Nikon microscope, using the x40 water-immersion objective, to acquire images of single myelinated nerve fibres.

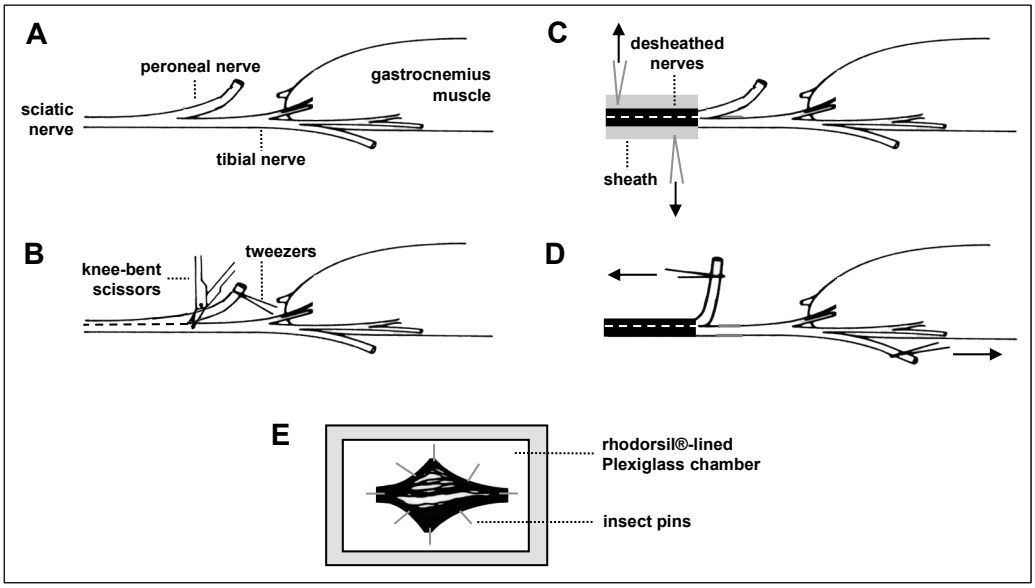

Fig. 1 Schematic representation of the dissection procedure of myelinated nerve fibres. (**A**) *Gastrocnemius* muscle innervated by the sciatic nerve comprising the peroneal nerve and the tibial nerve ending with several small branches. (**B**) Open the sheath of lamellar connective tissue with knee-bent scissors along the peroneal and tibial nerves, starting from an incision at the separation level of these two nerves. (**C**) Move the sheath to one side and cut it. (**D**) Pull away the peroneal nerve while simultaneously pulling the tibial nerve in the opposite direction. (**E**) Pin a de-sheathed piece of either the peroneal or the tibial nerve to the bottom of the Rhodorsil®-lined Plexiglas chamber and gently tease apart the myelinated nerve fibres to form a fan.

The study was conducted at room temperature (22-24°C) with the Sarastro-2000 confocal microscope (Fig. 2). FM1-43 was excited by the single 488 nm laser line (all-lines 12.5 mW) attenuated to 3 % by a neutral density filter. The emission of FM1-43 was detected through a dichroic beam splitter 510DRLP and two filters 510 nm and 535 nm long-pass. The aperture setting of the confocal pinhole was 100 µm and the photomultiplier tube ran at 600-850 V. In each experiment, this latter parameter was set at a constant level to give maximal signal without saturation. The fluorescence was thus converted first to an electrical signal and then to an 8-bit numerical signal, raster scanning producing the image.

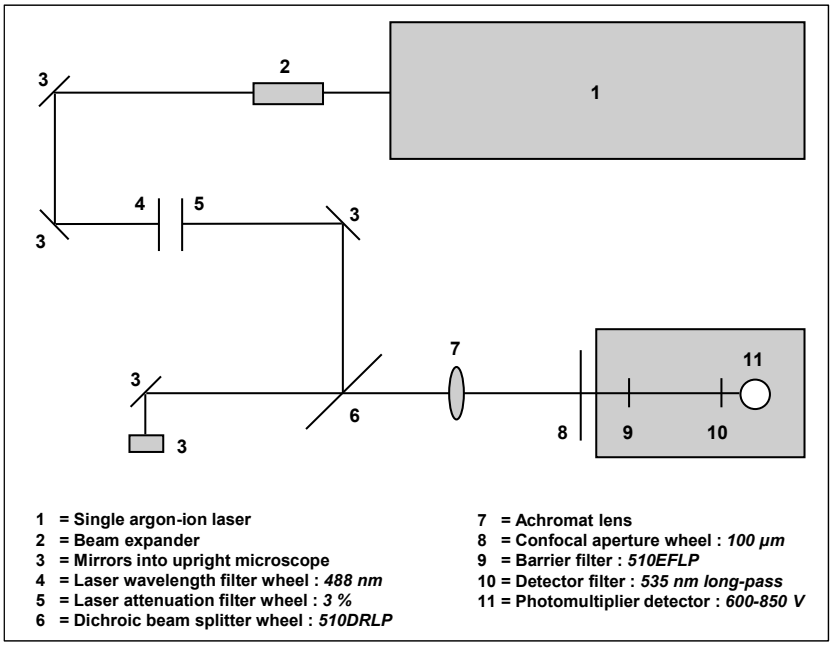

Fig. 2 Schematic representation of the Sarastro-2000 confocal laser scanning system. See text for more details.

The UNIX workstation, integrated into the Sarastro system, was used to control the scanner module and to process data. Series of usually 30 optical sections (Fig. 3A), scanned (without averaging) at 0.5 µm *z*-increments through a myelinated nerve fibre, were collected using a standard scanning format of 512 x 512 pixels (*x*-*y* pixel size equal to 0.5 x 0.5 µm).

4.4 Analysis procedure for images of myelinated nerve fibres

The workstation was also used for image analysis. For each optical series, a "look-through" projection was made using 16-bit maths: the algorithm essentially sums the thresholded intensities at each co-ordinate of the image stack, then simplifies to 8-bits in the final projection. The myelinated nerve fibre can be digitally reconstructed as a three-dimensional structure (Fig. 3B) with, nevertheless, asymmetric resolution: the format *x*-*y* plane has ~0.3 µm resolution but along the *z*-axis this is only ~1 µm. The projection is an in-focus representation of the nerve's contour.

Results were quantified on the same myelinated nerve fibre, before and during the various treatments, by measuring the internodal diameter, the nodal length (L) and the nodal diameter (D) on the "look-through" projection (Fig. 3C). The nodal volume (V) was then calculated as: $V = \pi L (D/2)^2$. Each parameter was determined as an average (mean ± S.E.M.) of at least 5 experimental measurements. Statistical analysis of data was performed using the Student's *t*-test (two-tailed). Data were considered significant at $P < 0.05$.

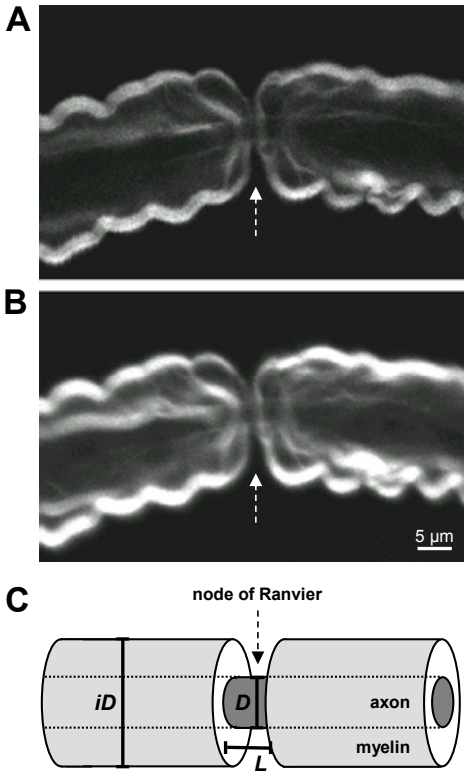

Fig. 3 Analysis procedure for images of myelinated nerve fibres. Images of an optical section (**A**) and a "look-through" projection calculated from a series of 30 optical sections scanned at 0.5 µm increments (**B**) through a myelinated nerve fibre stained with the FM1-43 dye. (**C**) Schematic representation of a myelinated nerve fibre. The simplest geometry of nodal and internodal parts of the fibre is assumed to correspond to co-axial cylinders. *L*, *D* and *iD* are, respectively, nodal length, nodal diameter and internodal diameter.

5. Results

Control experiments indicated that the staining procedure, described above, did not alter the physiology of nerve preparations [1, 2]. Moreover, this procedure consistently stained the various membrane structures of myelinated nerve fibres for several hours without destaining. Thus, the inability of the FM1-43 dye to cross nerve membranes, due to its partitioning only into the outer membrane leaflet [3], renders this dye particularly useful for imaging the morphology of myelinated nerve fibres. The myelin sheath layers, which surround the axons, stained brightly and the contours and edges of nodes of Ranvier, corresponding to the interruption of the myelin sheath layers, were well delineated. This is obvious in Fig. 4 (see also Fig. 3B), which shows images of three-dimensional reconstructions of FM1-43-stained myelinated nerve fibres. It is worth noting that the dye can cross nerve membranes of damaged myelinated nerve fibres.

Therefore, such myelinated nerve fibres, which consistently stained brightly, were unambiguously detected and rejected in the analyses (arrow in Fig. 4).

Under these conditions, changes in the volume of nodes of Ranvier could be easily observed if they occurred. This is exemplified by studying the effects of P-CTX-1B toxin, a potent voltage-dependent sodium channel activator (for a review, see [4]). In myelinated nerve fibres, this toxin produces a membrane depolarization which in turn triggers spontaneous and repetitive action potential discharges, due to the activation of sodium channels at the resting membrane potential where these channels are normally maintained in a closed state [1, 5].

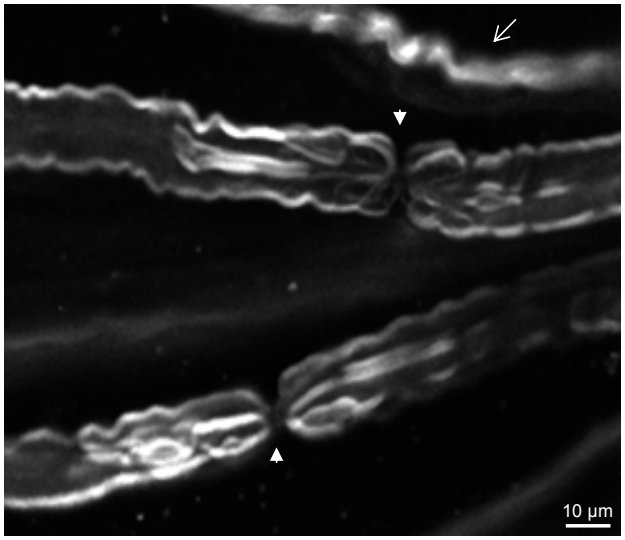

Fig. 4 Image of myelinated nerve fibres. Three-dimensional reconstructions by "look-through" projections calculated from series of 32 optical sections scanned at 0.5 µm increments through myelinated nerve fibres stained with the FM1-43 dye. The white arrow heads indicate the nodes of Ranvier and the arrow shows a damaged myelinated nerve fibre.

Fig. 5A shows images of three-dimensional reconstructions of a single myelinated nerve fibre, before and at various times after addition of 10 nM P-CTX-1B to the standard physiological solution. As shown in this typical experiment, the toxin produced a marked nodal swelling in a time-dependent manner.

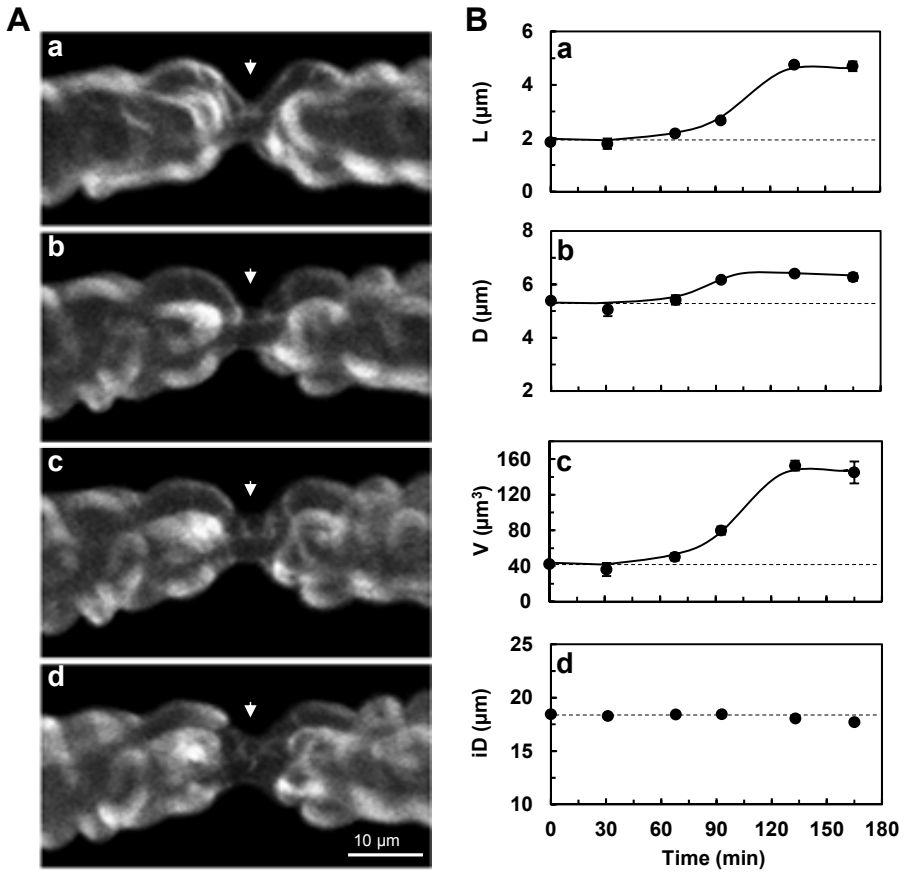

Fig. 5 Effect of P-CTX-1B on the morphology of a single myelinated nerve fibre. (**A**) Images of three-dimensional reconstructions by "look-through" projections of the same myelinated nerve fibre, stained with the FM1-43 dye, obtained under control conditions (**a**) and after 68 min (**b**), 93 min (**c**) and 133 min (**d**) treatment with 10 nM P-CTX-1B. In each case, a series of 30 optical sections was scanned at 0.5 µm increments through the myelinated nerve fibre. Notice the swelling of the node of Ranvier during the action of the toxin (white arrow heads). (**B**) Nodal length (*L*, **a**), nodal diameter (*D*, **b**), nodal volume (*V*, **c**) and internodal diameter (*iD*, **d**) determined from the myelinated nerve fibre imaged in A, before (time 0) and at different times after the addition of 10 nM P-CTX-1B to the external solution. Dotted lines indicate the value of parameters under control conditions. Morphological parameters were either measured (a, b and d) or calculated (c) as described in Fig. 3C. Means ± S.E.M. of at least 5 distinct determinations.

Quantification of this effect revealed that a statistically significant ($P< 0.05$) increase in the nodal length, in the nodal diameter, and consequently in the nodal volume, occurred during the action of P-CTX-1B (Fig. 5B). The toxin effect appeared about 60 min after the addition of P-CTX-1B to the external solution, was maximal after about 130 min exposure to the toxin and was well maintained during a further 30 min. At that time, an increase in the volume of the node of Ranvier of about 3-fold was detected with respect to controls (see Fig. 5Bc). The morphology of internodal parts of the myelinated nerve fibre, covered by myelin sheath layers, was apparently not altered during the action of P-CTX-1B (see Fig. 5A). Indeed, the internodal diameter of the fibre remained unaffected by the toxin (Fig. 5Bd), the small variations observed in that case being statistically not significant ($P> 0.05$).

The P-CTX-1B-induced nodal swelling of myelinated nerve fibres could be completely reversed by subsequent addition of 100 mM D-mannitol to the external solution containing the toxin. Indeed, the nodal volume of myelinated nerve fibres, previously increased by 10 nM P-CTX-1B to 216 ± 17 % (n = 16) with respect to controls, recovered 100 ± 11 % (n = 8) of control values after about 60 min exposure to D-mannitol, *i.e.* values statistically similar to those obtained before P-CTX-1B application (Fig. 6). When D-mannitol (100 mM) was first added to the external solution, in the absence of P-CTX-1B, the nodal volume of myelinated nerve fibres was significantly ($P< 0.05$) decreased, in less than 60 min, to 81 ± 11 % (n = 13) of control values. Under these conditions, the nodal volume was not significantly affected by the subsequent addition of P-CTX-1B (10 nM) applied for at least 120 min, *i.e.* it was 97 ± 13 % (n = 13) of control values (Fig. 6). These results indicate that hyperosmolar D-mannitol could not only reverse, but also prevented the increase in the nodal volume of myelinated nerve fibres caused by P-CTX-1B. The nodal volume was increased to 168 ± 28 % (n = 10) of control values when the myelinated nerve fibres were exposed to a toxin-free hypoosmolar solution, *i.e.* when the external concentration of NaCl was reduced by 50 % in the standard physiological solution (Fig. 6). This effect appeared within about 10 min and was stable after 30-60 min.

Finally, to ascertain that voltage-dependent sodium channels were involved in the nodal swelling induced by P-CTX-1B, myelinated nerve fibres were exposed first to the sodium channel blocker TTX (1 µM) for about 120 min and then to P-CTX-1B (10 nM) in the continuous presence of TTX for additional 120 min. As shown in Fig. 6, no significant change was detected on the nodal volume of myelinated nerve fibres under these conditions. The calculated nodal volume, expressed with respect to control, was 95 ± 4 % (n = 12) in the presence of TTX and 92 ± 5 % (n = 12) after P-CTX-1B addition to the TTX-containing solution.

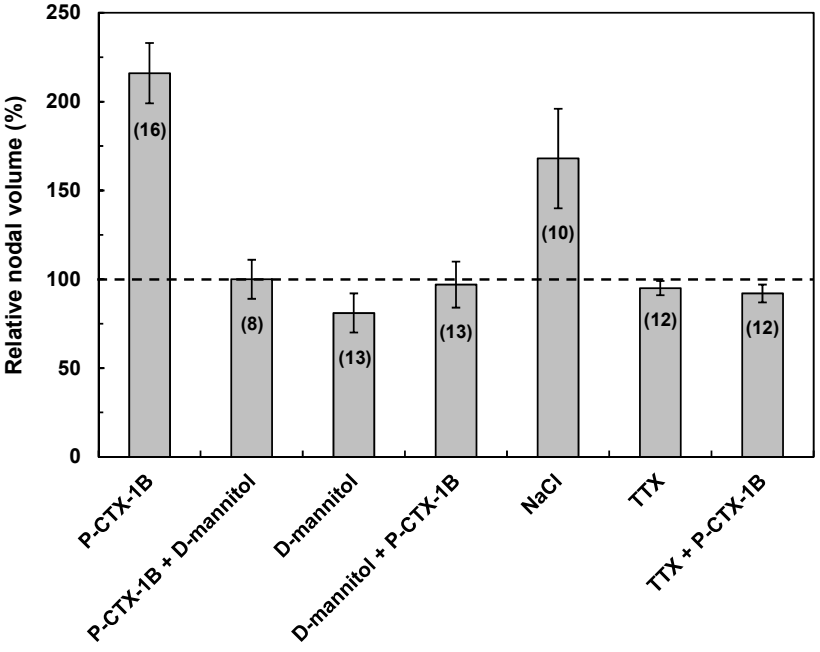

Fig. 6 Effects of P-CTX-1B (10 nM), D-mannitol (100 mM), a reduced (by 50 %) external NaCl concentration and TTX (1 µM) on the nodal volume of myelinated nerve fibres. Steady-state values of nodal volume calculated from myelinated axons exposed (1) to P-CTX-1B for at least 120 min and then to D-mannitol added to the toxin-containing medium for about 60 min; (2) to D-mannitol for about 60 min and then to D-mannitol and P-CTX-1B for at least 120 min; (3) to a reduced external concentration of NaCl for about 60 min; or, (4) to TTX for about 120 min and then to P-CTX-1B in the continuous presence of TTX for an additional 120 min. The nodal volume was expressed with respect to its control value (dotted line) determined in the standard physiological solution. Mean ± S.E.M. of 8-16 myelinated nerve fibres (number in parentheses).

We also observed a marked swelling of nodes of Ranvier, without apparent modification in the morphology of internodal parts of myelinated nerve fibres, with two other Pacific ciguatoxins, P-CTX-4B and P-CTX-3C purified from the wild toxic *Gambierdiscus toxicus* dinoflagellate and poisonous moray eels (*Gymnothorax javanicus*) respectively [6, 7], with a Caribbean ciguatoxin, C-CTX-1 extracted from the poisonous pelagic fish *Caranx latus* [8], and with two brevetoxins, PbTx-1 and PbTx-3 purified from the cultured *Gymnodinium breve* dinoflagellate [7]. In each case, the effect of the toxin was prevented and/or reversed by hyperosmolar D-mannitol and was antagonized by the blockade of voltage-dependent sodium channels with TTX.

It is well known that ciguatoxins and brevetoxins, by binding to the receptor-site 5 of voltage-dependent sodium channels, produce a persistent activation of these channels at the resting membrane potential, thus increasing the resting membrane sodium permeability of target cells, *i.e.* enhancing the entry of sodium ions into excitable cells (for reviews,

see [4, 9, 10]). Such an enhanced entry of sodium ions into axons has been shown to depolarize the nodal membrane and consequently to induce the appearance of spontaneous and repetitive action potential discharges in myelinated nerve fibres.

Using confocal laser scanning microscopy and passive staining with the styryl dye FM1-43, we could show that ciguatoxins and brevetoxins also produce a nodal volume increase in a single living myelinated nerve fibre. The fact that this increase was antagonized by blocking voltage-dependent sodium channels with TTX supports the view that the nodal swelling, produced by these dinoflagellate toxins, originates by an enhanced sodium ions entry into axons through TTX-sensitive sodium channels opened both at the resting membrane potential and during spontaneous and repetitive action potential discharges. Such an entry will lead to an increased internal concentration of sodium ions that is expected to raise the internal osmolality enough to disturb the osmotic equilibrium between intra- and extra-axonal media, causing an influx of water that will be responsible for the long-lasting nodal swelling of myelinated nerve fibres. The water movements occurring across the nodal membrane, which are dependent on osmotic pressure gradients, may be necessary to restore both the osmotic equilibrium and the internal concentration of sodium ions to their initial level. That hyperosmolar D-mannitol prevented and/or reversed the toxin-induced nodal swelling further supports the view that such a swelling is related to osmotic changes since external hyperosmotic solutions are expected to cause water movements from the intra- to the extra-axonal compartment, as evidenced by the nodal shrinkage of toxin-untreated myelinated nerve fibres bathed in an external solution containing hyperosmolar D-mannitol.

These results are of particular interest since (i) they indicate that changes in cellular volume may occur after activation of voltage-dependent ion channels under isoosmotic conditions and (ii) they provide a scientific basis for understanding the beneficial action of hyperosmolar D-mannitol when used in the clinical treatment of ciguatera fish poisoning ([11]).

6. Discussion

This paper reports how to use the styryl dye FM1-43, confocal laser scanning microscopy and digital three-dimensional image analysis for axonal volume measurements at the node of Ranvier of living myelinated nerve fibres. An application to the description of the changes that occur in the nodal volume of a single fibre, during the action of a ciguatoxin, exemplifies the use of these methods.

Styryl dyes, such as FM1-43, were originally developed as membrane-potential sensors and then have also proven extremely useful as tools for studying exocytosis, endocytosis and trafficking of endosomes, especially recycled synaptic vesicles, in living cells [3, 12]. In addition, FM1-43 can also be used to passively and accurately stain the plasma membranes of various living nerve preparations including motor nerve terminals [2, 13], neuroblastoma cells [13, 14] and myelinated nerve fibres as reported in the present paper. It appears that FM1-43 inserts into the membrane *via* its lipophilic tail (two aliphatic chains) with the pyridinium dicationic head anchored at the surface and an aromatic nucleus between the two. The anchor prevents free diffusion to other membranes except essentially by membrane flow (endocytosis, exocytosis, vesicle formation, etc.). Indeed, once intracellular compartments are labelled by such processes, the plasma membrane component can, if desired, be substantially reduced by extended washing, leaving the intracellular compartment visible. Image contrast is enhanced by the fact that the quantum yield of FM1-43 is far higher in the lipid environment than in water. However, the spectral properties due to the fluorescent aromatic nucleus depend strongly on the membrane micro-environment and may be different for various tissues: spectroscopy in pure solutions is quite misleading for *in vivo* studies. For instance, in methanol FM1-43 has an excitation peak at 502 nm with emission at 625 nm (red), whereas in the present system we use 488 nm excitation and the emission is yellow (~570 nm). Where this strategy is to be used in tissue expressing GFP, one may adopt the analogous FM4-64 whose emission in biological membranes is red, well away from GFP [15].

Confocal laser scanning microscopy is a point illumination/point detection technique, in which light deriving from out-of-focus specimen regions is greatly minimised, if not suppressed. This property and the use of a large numerical aperture lens provide better resolution, contrast and depth discrimination than a conventional widefield microscope. Therefore, it allows optical sectioning of in-focus planes through the depth of the myelinated nerve fibre and digital three-dimensional image recordings, which simplifies subsequent quantitative analyses (see [16]). Under these conditions, it is possible to detect and quantify, as a function of time, the changes that occur in the nodal volume of a single living myelinated nerve fibre.

Laser light intensity and photomultiplier detector voltage should be carefully adjusted so that the images have a signal-to-noise ratio as high as possible, *i.e.* a high intensity of specific staining and a low intensity of background, without pixel saturation. However, the laser intensity of the incident light should not be higher than reported here since this will produce not only membrane damage but also a fading with repeated imaging due to FM1-43 photobleaching, *i.e.* a decrease of its fluorescence, although the fluorophore is generally considered to be highly photostable [12]. For the same reason, the high-pressure lamp of the epifluorescence microscope is attenuated and used with moderation. Such membrane damage and photobleaching, which in turn will decrease the signal-to-noise ratio, may be also reduced by minimising exposure times. It is recommended to make single optical sections as test scans of the myelinated nerve fibre to establish the appropriate adjustment of laser light intensity and photomultiplier detector sensitivity. When these

parameters have been determined, they must be kept constant between serial recordings from a given control and treated fibre to allow comparison between the obtained images. The exact start focal plane is determined with the best accuracy by exploring single scans around the lower border of the myelinated nerve fibre.

7. Conclusion

In conclusion, confocal laser scanning microscopy and the use of the styryl dye FM1-43 provide a reliable methodology for axonal morphometry of a node of Ranvier in a single living myelinated nerve fibre. This allows accurate detection and quantification of dynamic morphological changes, to address the relation existing between morphology and functional characteristics.

Acknowledgements This research was funded, in part, by grant Aquaneurotox ANR-12-ASTR-0037-01 from the Agence Nationale de la Recherche (France).

References

[1] Benoit E, Juzans P, Legrand AM, Molgó J. Nodal swelling produced by ciguatoxin-induced selective activation of sodium channels in myelinated nerve fibers. Neuroscience. 1996; 71:1121-31.

[2] Molgó J, Juzans P, Legrand AM. Confocal laser scanning microscopy: a new tool for studying the effects of ciguatoxin (CTX-1b) and mannitol at motor nerve terminals of the neuromuscular junction *in situ*. Memoirs of the Queensland Museum. 1994; 34:577-85.

[3] Hoopmann P, Rizzoli SO, Betz WJ. Imaging synaptic vesicle recycling by staining and destaining vesicles with FM dyes. Cold Spring Harb Protoc. 2012; 2012:77-83.

[4] Lewis RJ, Molgó J, Adams D. Ciguatera toxins: Pharmacology of toxins involved in ciguatera and related fish poisonings. In: Botana L, editor. Seafood and Freshwater Toxins. New York: Marcel Dekker; 2000. Chapter 20, p. 419-47.

[5] Benoit E, Legrand AM, Dubois JM. Effects of ciguatoxin on current and voltage clamped frog myelinated nerve fibre. Toxicon. 1986; 24:357-64.

[6] Mattei C, Benoit E, Juzans P, Legrand AM, Molgó J. Gambiertoxin (CTX-4B), purified from wild *Gambierdiscus toxicus* dinoflagellates, induces Na^+-dependent swelling of single frog myelinated axons and motor nerve terminals *in situ*. Neurosci. Lett. 1997; 234:75-8.

[7] Mattei C, Dechraoui MY, Molgó J, Meunier FA, Legrand AM, Benoit E. Neurotoxins targeting receptor site 5 of voltage-dependent sodium channels increase the nodal volume of myelinated axons. J. Neurosci. Res. 1999; 55:666-73.

[8] Mattei M, Molgó J, Marquais M, Vernoux JP, Benoit E. Hyperosmolar D-mannitol reverses the increased membrane excitability and the nodal swelling caused by Caribbean ciguatoxin-1 in single frog myelinated axons. Brain Res. 1999; 847:50-8.

[9] Meunier FA, Mattei C, Molgó J. Marine toxins potently affecting neurotransmitter release. Prog. Mol. Subcell. Biol. 2009; 46:159-86.

[10] Mattei C, Legros C. The voltage-gated sodium channel: a major target of marine neurotoxins. Toxicon. 2014; 91:84-95.

[11] Friedman MA, Fleming LE, Fernandez M, Bienfang P, Schrank K, Dickey R, Bottein MY, Backer L, Ayyar R, Weisman R, Watkins S, Granade R, Reich A. Ciguatera fish poisoning: treatment, prevention and management. Mar. Drugs. 2008; 6:456-79.

[12] Betz WJ, Mao F, Smith BS. Imaging exocytosis and endocytosis. *Curr. Op. Neurobiol.* 1996; 6:365-71.

[13] Mattei C, Molgó J, Benoit E. Involvement of both sodium influx and potassium efflux in ciguatoxin-induced nodal swelling of frog myelinated axons. Neuropharmacology. 2014; 85:417-26.

[14] Benoit E, Meunier FA, Mattei C, Juzans P, Legrand AM, Molgó J. Do sodium ion influx through ciguatoxin-modified voltage-dependent sodium channels induce swelling of the myelinated nerves and neuroblastoma cells? In: Reguera B, Blanco J, Fernández ML, Wyatt T, editors. Harmful Algae. Xunta de Galicia and Intergovernmental Oceanographic Commission of UNESCO; 1998. p. 590-3.

[15] Haugland RP. Handbook of fluorescent probes and research chemicals. Molecular Probes. Eugene, Oregon, USA; 1996. p. 408-12.

[16] Wallén P. Three-dimensional reconstruction of fluorescence-labeled neurons in the lamprey central nervous system, using a confocal laser scanning microscope. NeuroProtocols. 1993; 2:83-91.